LBL-33731
UC-414

Lawrence Berkeley Laboratory
UNIVERSITY OF CALIFORNIA

Accelerator & Fusion Research Division

Presented at the Computational Accelerator Physics Conference, Pleasanton, CA, February 22–26, 1993, and to be published in the Proceedings

Numerical Simulation of Relativistic Klystrons

G. Fiorentini

February 1993

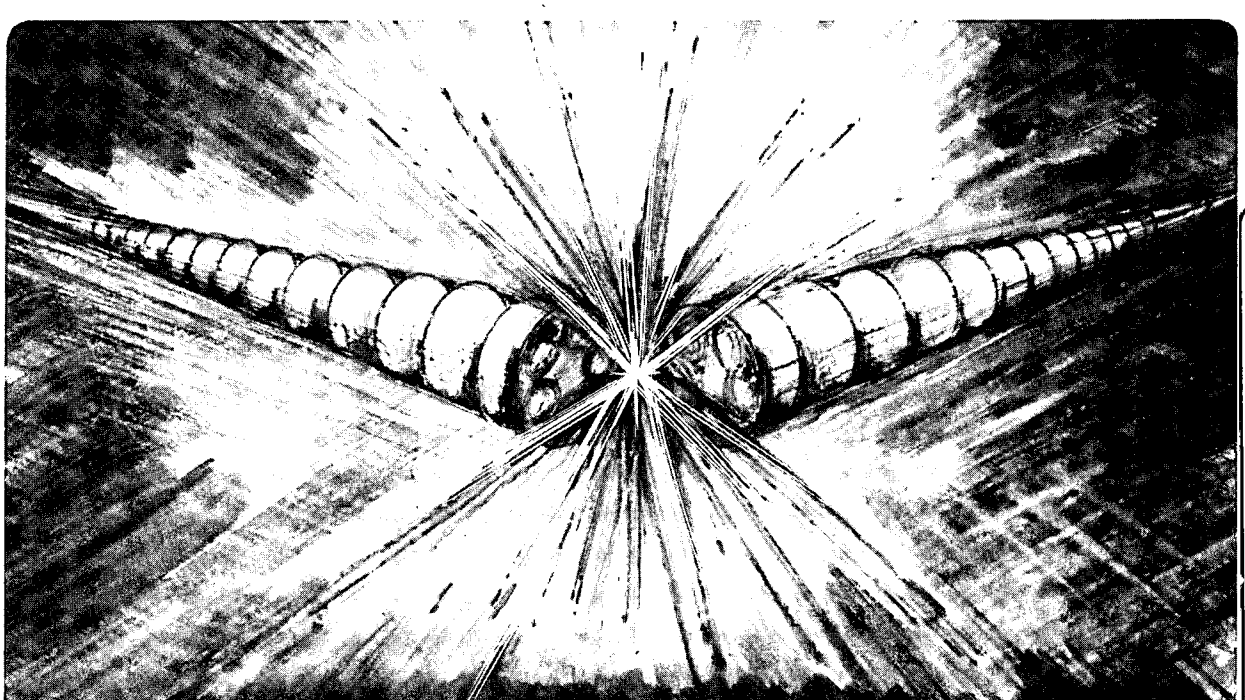

Prepared for the U.S. Department of Energy under Contract Number DE-AC03-76SF00098

DISCLAIMER

LBL-33731
CBP-1
UC-414

Numerical Simulation of Relativistic Klystrons

Giulia Fiorentini*

Lawrence Berkeley Laboratory, University of California, Berkeley, California 94720

February 1993

*Work supported by the Director, Office of Energy Research, Office of High Energy and Nuclear Physics, Division of High Energy Physics, of the U.S. Department of Energy under Contract No. DE-AC03-76SF00098

Numerical Simulation of Relativistic Klystrons*

Giulia M. Fiorentini†
Lawrence Berkeley Laboratory,
University of California, Berkeley,CA 94720

ABSTRACT

The Microwave Source Facility at the Lawrence Livermore National Laboratory is a facility for testing high power microwave devices for possible linear collider applications. In order to study the feasibility of a Relativistic Klystron/Two Beam Accelerator concepts, we are planning a series of experiments that involve reacceleration of a modulated beam alternating with power extraction. In support of these planned experiment, we have performed numerical simulations using the two-dimensional, time-dependent code RKS2. We describe the main features of RKS2 and present simulation results including analysis of beam transport, modulation, phase space and power extraction.

I. Introduction

In a relativistic klystron we extract energy from a relativistic beam of electrons and feed the resonant mode in the RF band for which the klystron is built. The RKS2 code studies the interaction of a charged particle beam with an electromagnetic wave in a relativistic klystron.

This code models only cylindrically symmetric problems. Only two coordinates (r,z) are necessary to describe forces since they are assumed to be cylindrical symmetric. Each particle is a charged point with longitudinal position, radius and an angle. The angular distribution is uniform. The source code is designed to be able to model several different combinations of standing wave (SW) cavities, traveling wave (TW) tubes, drift tubes, potential gaps, transverse kick cavities and others components.

In section II we describe the physics of the code, while in section III a particular application is presented.

II. The Physics of the Code

The code solves a system of 2nd order differential equations to compute the current density from the fields and the fields from the current density.

---

* This work was supported by the Director, Office of Energy Research, Office of Basic Energy Sciences Division, of the U.S. Department of Energy under Contract No. DE-AC03-76SF00098.

† Permanent address: Universita' Statale Milano, Via Celoria 18 , Milano, Italy.

The system of equations comes from the waves equation

$$\nabla^2\vec{E}_n - \frac{1}{c^2}\frac{\partial^2\vec{E}_n}{\partial t^2} = \frac{4\pi}{c^2}\vec{J} \qquad \text{(II.1)}$$

where n is an index for which cavity is considered, and from the motion equations as function of z:

$$\frac{dx}{dz} = {}^{v_x}\!/_{v_z}\,, \qquad \frac{dy}{dz} = {}^{v_y}\!/_{v_z}\,, \qquad \frac{dy}{dz} = {}^{v_y}\!/_{v_z}$$

$$\frac{d\psi}{dz} = {}^{\omega}\!/_{v_z}\,, \quad \frac{dv_x}{dz} = \frac{qm}{\gamma}\cdot\left[\vec{E} + \vec{v}\times\vec{B}\right]_x\,, \quad \frac{dv_y}{dz} = \frac{qm}{\gamma}\cdot\left[\vec{E} + \vec{v}\times\vec{B}\right]_y\,. \qquad \text{(II.2)}$$

The code computes the Lorentz force from all the electromagnetic fields acting on the particles: space charge , microwave and focusing fields, and also longitudinal accelerating fields, transverse kicks and so on.

1. THE CIRCUIT EQUATION

Assuming that a single cavity mode is dominant, the fields ringing in a cavity can be expressed as the product of a slowly varying time dependent term, a position **r** dependent term and a phase term :

$$\vec{E}_n(\mathbf{r},t) = f_n(t)\cdot\vec{E}_n(\mathbf{r})\cdot\exp(-j\omega t) \qquad \text{(II.3)}$$

n is an index for the cavity, ω is the frequency of the driving field or current depending on whether the cavities are fed by an electromagnetic wave or by an RF current, and usually is equal to the resonant frequency (but it only needs to be close to the resonance frequency) and $\vec{E}_n(\mathbf{r})$is the normalized eigenmode that has been excited . The eigenvalue and the eigenmode depend on the geometry of the cavity and are part of the input data for the RK codes. $f_n(t)$ is the dynamic amplitude of the field that is solved through the circuit equation, obtained by substituting eq. (II.3) into (II.1) and integrating over the volume of the n^{th} cavity. Here below the result:

$$\ddot{f}_n + \left(\frac{\omega_n}{Q_n} - 2j\omega_n\right)\dot{f}_n + \left(\omega_n^2 - \omega^2 - \frac{j\omega\omega_n}{Q_n}\right)f_n -$$

$$\left(\; K_n^{n-1} f_{n-1} + K_n^{n+1} f_{n+1}\;\right) = \frac{j\omega}{\varepsilon_0}\int dV_n\cdot\vec{E}_n{}^*\cdot\vec{J} \qquad \text{(II.4)}$$

with

$$\frac{\omega_n{}^2}{c^2} = \int dV_n\left|\vec{\nabla}\times E_n(r,z)\right|^2, \qquad \text{(II.5)}$$

and

$$K_n^{n-1} = c^2 \int_{S_{n-1/n}} d\bar{S} \cdot \left[\bar{E}_n^* \times \left[\bar{\nabla} \times \bar{E}_{n-1} \right] \right] \quad . \qquad \text{(II.6)}$$

The code solves for the value of the term $f_n(t)$ (n=1,...N), as a function of the current density J, the amplitude $\bar{E}_n(\mathbf{r})$; the code need to be supplied with the value of Q_n (the quality factor of the cavity n), $K_{n,n-1}$ and $K_{n,n+1}$ (the coupling terms between the cavity n and the cavity n-1 and n+1: they are zero in case n represents a SW cavity), and ω_n that comes out to be the resonant frequency for SW cavity, while coincides with the frequency of the $\pi/2$ mode for a traveling wave cavity.

2.THE PREPROCESSOR TO CONVERT SW -MODES INTO TW -MODES

Before running RKS2 we use Superfish to determine the resonant frequency and the vector potential of the mode with which we are concerned. By knowing the vector potential the code solves for the electric field and the magnetic field. For TW structures another step is required before to running RKS2. A preprocessor turns SW modes into TW modes[1]. Furthermore it furnishes the group velocity from computing the rate between the power flux through one surface and the energy stored per unit length:

$$v_g = \frac{P}{W_{TW}} = \frac{\frac{1}{2}\int E_r \cdot H_\phi \, ds}{\int_{\text{unit length}} \varepsilon \frac{E^2}{2} \, dV + \int_{\text{unit length}} \mu \frac{H^2}{2}} \qquad \text{(II.7)}$$

3. HOW TO COMPUTE ω_n AND THE COUPLING FACTORS.

For a SW cavity at steady state, with no beam, the circuit eq. becomes

$$\left(\omega_n^2 - \omega^2 - \frac{j\omega\omega_n}{Q_n} \right) f_n = 0 \qquad \text{(II.8)}$$

If Q_n is very large we can neglect the term $\frac{j\omega\omega_n}{Q_n}$ in eq. (II.8) and ω_n coincides with the resonant frequency. For a TW cavity to determine the value of ω_n let us consider the circuit equation at steady state and with driving current J=0. The equation becomes

$$\left(\omega_n^2 - \omega^2 - \frac{i\omega\omega_n}{Q_n} \right) f_n - \left(K_n^{n-1} f_{n-1} + K_n^{n+1} f_{n+1} \right) = 0. \qquad \text{(II.9)}$$

As above we will omit $\frac{j\omega\omega_n}{Q_n}$ with respect to $\omega_n^2-\omega^2$.

We obtain

$$(\omega_n^2-\omega^2)f_n-\left(\ K_n^{n-1}f_{n-1}+K_n^{n+1}f_{n+1}\ \right)=0 \qquad \text{(II.10)}$$

If we consider an infinite structure the coupling terms are all the same, and for Flouquet theorem the fields only differ by a factor of phase. So we can write:

$$\left(\omega_n^2-\omega^2\right)f_n-\left(\ K\ f_n\cdot e^{i\delta\cdot\ell}+K\ f_n\cdot e^{-i\delta\cdot\ell}\ \right)=0, \qquad \text{(II.11)}$$

and

$$\omega_n^2-\omega^2=2\cdot K\cos(\delta\,\ell), \qquad \text{(II.12)}$$

where the formula (II.12) is a simple version of the dispersion relation. Moreover it says that for $\omega=\omega_n$ the phase advance is $\pi/2$.
After a differentiation, we obtain

$$\frac{d\omega}{d\delta}=\frac{K}{\omega}\cdot\ell\sin(\delta\,\ell), \qquad \text{(II.13)}$$

where the left hand size is the group velocity.

Since from Superfish we know the frequency ω, phase advance δ for a certain mode, the length ℓ of the cavity and from the preprocessor we know the group velocity, equation (II.13), can be used to calculate the coupling factor K . Substituting ω, δ, K in (II.12) we find out ω_n to input to the code.

4.THE FOCUSING MAGNETIC FIELD AND THE CONSERVATION OF CANONICAL MOMENTUM.

There are two different ways to specify the magnetic field along the klystron: reading an input data file or giving the geometry of the solenoids. The code also takes into account what magnetic path the beam takes as it goes from the cathode to the entrance of the structure. It is well know that if a beam goes through a non uniform magnetic field by the time it reaches the entrance it has gotten a certain angular momentum (from the conservation of the canonical angular momentum). This helps the beam to be constrained.

This law is also expressed in the envelope equation:

$$\ddot{R}+K_\beta^2R-\frac{K}{2R}-\frac{\varepsilon^2+\left(q\psi_0/p\right)^2}{R^3}=0. \qquad \text{(II.14)}$$

where R=rms radius=$\sqrt{< r^2 >}$, $K_\beta = \frac{eB_z}{2\gamma\beta mc}$, K=perveance=$\frac{2I/I_0}{(\beta\gamma)^3}$,

I_0=17000amp, ψ_0=magnetic flux enclosed within the beam at the source.

If the beam at the source is subject to no magnetic field, $\psi_0$is zero in the eq.(II.13). If the beam at the source is subject to a non zero magnetic field, ψ_0 is non zero and in the envelope equation we need to add to the real emittance term the additional $\frac{(q\psi_0/p)^2}{R^3}$ to get the effective emittance of the beam. This is one of the features the code supplies if we input the value of the magnetic field at the cathode.

III. An Application: The Reacceleration Experiment

A collaboration between the Lawrence Livermore National Laboratory and the Lawrence Berkeley Laboratory has been studying microwave sources which could be suitable drivers for a future TeV linear e^+e^- collider. The Choppertron[2], a high-power microwave generator which uses transverse modulation of the drive beam, has been successfully tested at the Microwave Source Facility[3]. Although the Choppertron has demonstrated high-power pulses, >150 MW per output at 11.424 GHz with stable phase and amplitude and >400 MW total peak power, the conversion efficiency of beam energy to microwaves is only about 30%. The efficiency could be significantly improved by adding up more and more TW structures for the power extraction and reaccelerating the beam after each extraction unit. Besides the energy of the beam has been increased (5Mev) to reduce the space charge effect. The application of this concept to a linear collider is referred to as the Relativistic Klystron Two-Beam Accelerator (RK-TBA)[4].

Fig. 1 shows a layout of the proposed reacceleration experiment. The major experimental components, except for the induction accelerator that generates the drive beam, are shown in the layout. These components include the Choppertron beam modulator, traveling-wave microwave extraction structures, and induction cells for reacceleration.

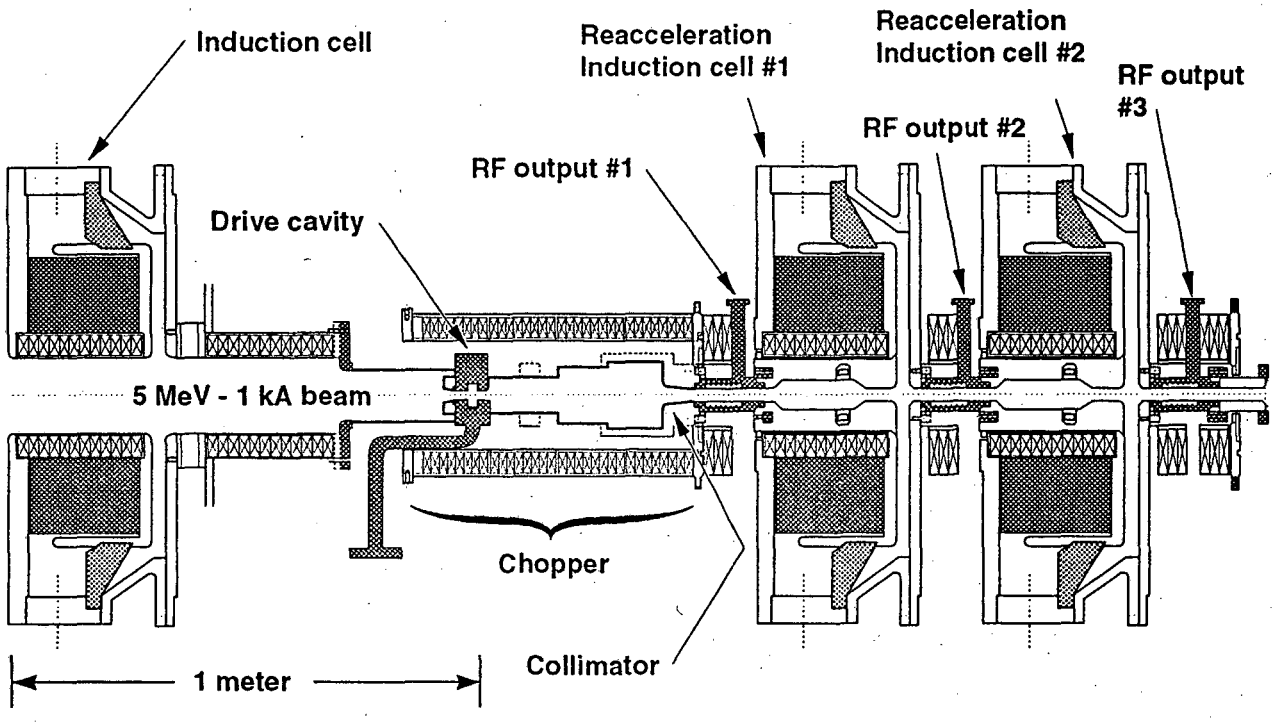

Figure 1. Schematic of proposed reacceleration experiment.

The RKS2 code has been used to simulate the beam transport and the field dynamics. As mentioned before it only deals with cylindrically symmetric fields, and transverse instabilities has been studied separately. We shall not describe the experiment here , as that has been described elsewhere[5,6] but simply show how RKS2 has been helpful. we shall separately talk about the modulation section and the extraction section.

1. THE MODULATOR SECTION

The choppertron modulator has been analyzed elsewhere[5,6]. We will just introduce the geometry and the way it works: In a dipole cavity an alternated kick (f=5.712Ghz) is given to the beam. The beam is allowed to oscillate in a drift region of uniform magnetic field. After a length=$\lambda_\beta/4$, where

$$\lambda_\beta = \frac{4\pi\gamma\beta mc}{eB_z} \qquad \text{(III.1)}$$

is the betatron wavelength, the beam has reached a maximum deflection from the axis. At this point a collimator chops the beam resulting in a current modulation at twice the kick frequency. The condition

$$\text{drift length}=\lambda_\beta/4 ,$$

furnishes the best rf/dc ratio. Since the drift length is fixed eq.(III.1) determines the magnetic field that optimizes the deflection. For a 5Mev beam, the value of B_z that satisfies eq.(III.1) for our geometry is B_z=1kG. The choppertron was designed for 1kA of dc current and a normalized emittance $\varepsilon_N=30\pi$ cm mrad.

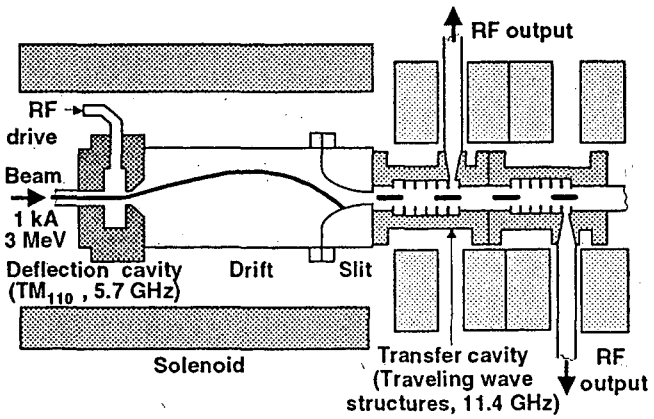

Figure 2. Schematic of the original Choppertron.

From the envelope equation (II.14) we set $\ddot{R}=0$ to determine the radius of the matched beam. The design envelope radio was R=4mm. In the real experiment the beam actual emittance was different ,

$\varepsilon_N \approx 100\pi$ cm mmrad. With this value of emittance it was not possible to match the beam (for an acceptable R value) keeping B_Z=1KG.

2. OPTIMIZATION OF PARAMETERS IN THE MODULATOR .

The use of RKS2 allowed us to determine the optimum choice of the following parameters , I, B_z, ε_n , R, to get the maximum rf current coming out of the modulator. The value of emittance depends upon the value of dc current. The higher is the dc current, the larger is the emittance. As a consequence beyond a certain value of dc current ($1\approx$kA) the benefit of having an intense beam is canceled by the disadvantage of having a larger emittance. From the value of magnetic field two parameters depend through inverse proportionality: the deflection and the radius of the envelope. From the deflection the rf current depends according to direct proportionality. From the envelope radius R the rf current depends according to some inverse proportionality law. There must be a middle value that optimizes the rf current.

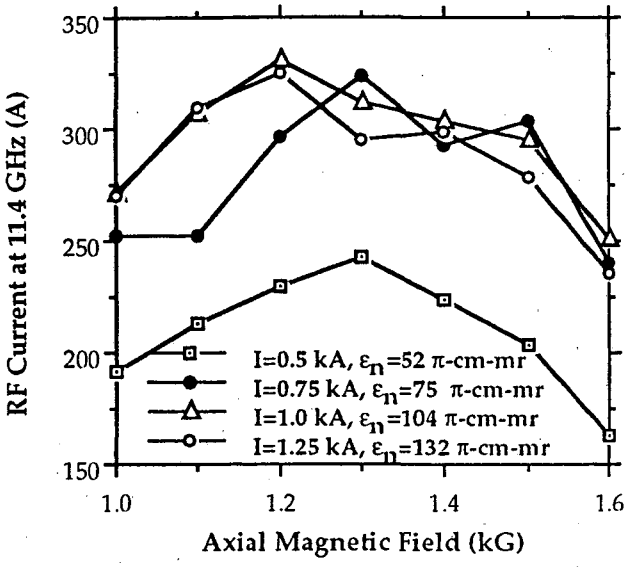

Figure 3. Predicted rf current for different beam emittances and dc currents, and fixed drive level = 1.2 MW.

In Fig.3 we show the result of series of simulations. Each curve has been obtained running RKS2 up to the end of the collimator and for different values of initial current. Each point of these curves has been obtained by running the code with different magnetic fields. The code produces in an output file the value of the dc current and the first two harmonics as a function of the longitudinal position. Besides for the analysis of the transient time it is possible to plot these variables at a fixed longitudinal position as a function of time. We chose to work with I=1.0kA, consequent $\varepsilon_N=100\pi$ cm mmrad, B_z =1.2kG, R=0.568cm.

3. BEAM TRANSPORT IN THE GAIN SECTION.

The RKS2 analyzes the beam transport . Plots of the current harmonics versus z, plots of the profile of the beam, plots of the radius of the envelope , plots of the longitudinal phase space were available. In Fig.6 we show the power extracted by TW#1, TW#2, TW#3. The big particle loss that is fingered by the most left arrow in Fig.4 has been attributed to a defocusing effect of the TW transverse fields. The beam profile plotted in Fig.5&7 show at different z how the later particles of each bucket receive a defocusing kick and how the earlier particles receive a focousing kick inside the first TW structure.

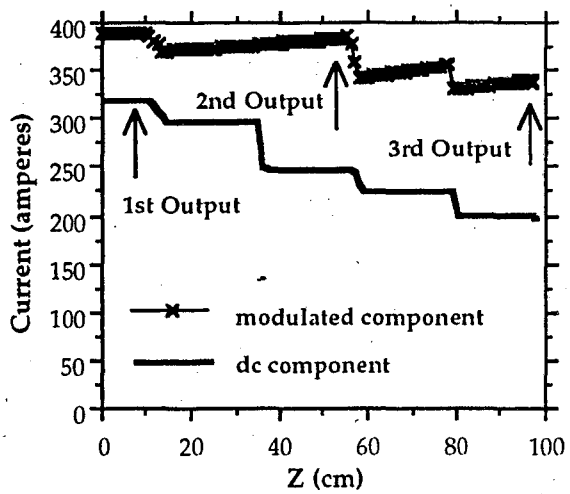

Figure 4. RF and DC current versus z.

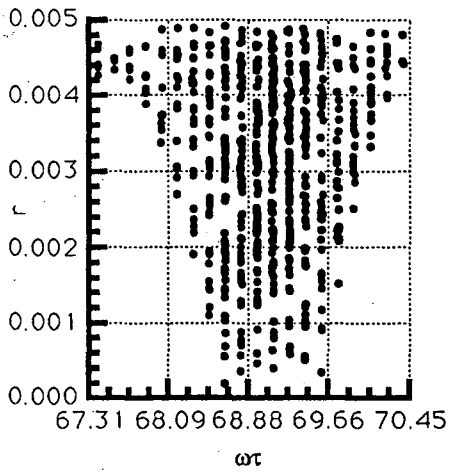

Figure 5. Profile r(m) of 1 bucket at the entrance of the first TW tube.

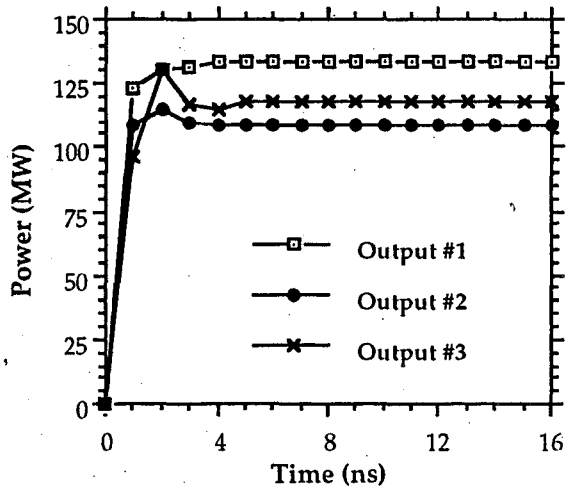

Figure 6. Power out versus time in the extraction cavities.

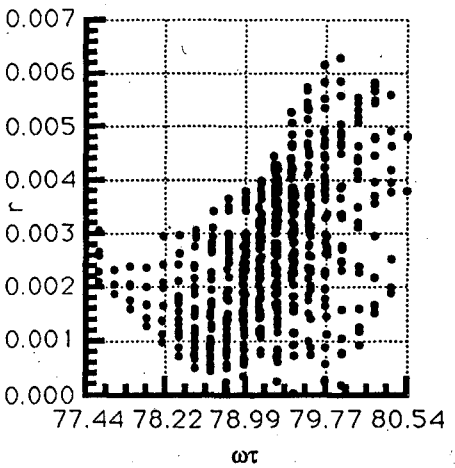

Figure 7. Profile r(m) of 1 bucket at the exit of the first TW tube.

In fig.8 as a verification of this effect we show the beam radius behavior versus z in the first TW structure and what it would be if we replaced the TW tube with a simple drift tube. In the second case the radius would reduce. In Fig.9 finally we show the rms radius expansion inside the pipe.

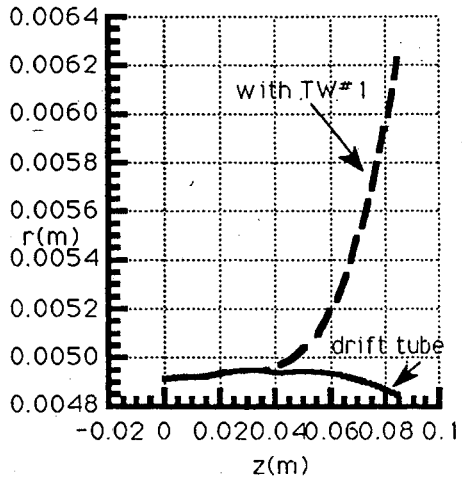

Figure 8. envelope radius versus z.

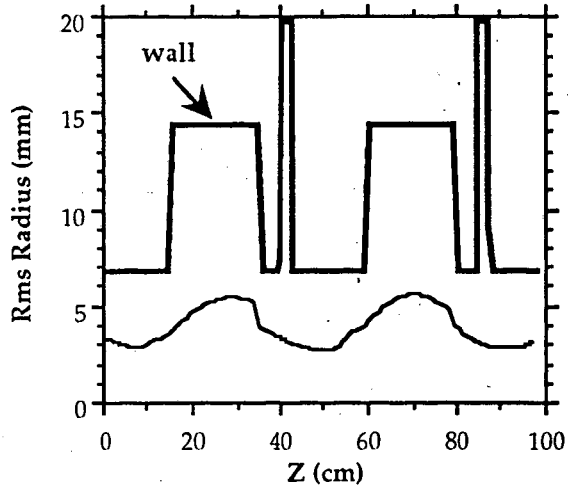

Figure 9. Rrms radius versus z.

IV. Acknowledgments

I would like to thank Tim Houck, Rob Ryne, and Andrew Sessler for their helpful suggestions and comments.

VI. References

1 G.A. Loew, R.H. Miller, R.A., "Computer Calculatios Of Travelling-Wave Periodic Structure Properties"

2 J. Haimson and B. Mecklenburg, "Design and Construction of a Chopper Driven 11.4 Ghz Traveling Wave RF Generator", Proceedings of the 1989 IEEE Particle Accel. Conf.,pp243-245.

3 T.L.Houck et al., "Relativistic Klystron Research for Two-Beam Accelerators," SPIE Symposium onIntense Microwave and Particle Beams II Proceedings Vol 1629-47 (1992).

4 A.M.Sessler and S.S. Yu, "Relativistic Klystron Version of the Two-Beam Accelerator,"Phys.Rev.Lett.,58,2439,1987.

5 T.L.Houck and G.A. Westnenskow, " Status of an Induction Accelerator Driven, High Power Microwave Generator at Livermore," Spie Proceedings Vol 1872-16,1993

6 G. M. Fiorentini, T. L. Houck, and C. Wang,"Design of a Reacceleration Experiment " SPIE proceedings 1993, Vol 1872-17,1993

LAWRENCE BERKELEY LABORATORY
UNIVERSITY OF CALIFORNIA
TECHNICAL INFORMATION DEPARTMENT
BERKELEY, CALIFORNIA 94720